

Expression of Progesterone Receptor Membrane Component-2 Within the Immature Rat Ovary and Its Role in Regulating Mitosis and Apoptosis of Spontaneously Immortalized Granulosa Cells¹

Daniel Griffin,^{3,5} Xiufang Liu,⁴ Cindy Pru,⁶ James K. Pru,⁶ and John J. Peluso^{2,4,5}

⁴Department of Cell Biology, University of Connecticut Health Center, Farmington, Connecticut

⁵Department of Obstetrics and Gynecology, University of Connecticut Health Center, Farmington, Connecticut

⁶Center for Reproductive Biology, Department of Animal Science, Washington State University, Pullman, Washington

ABSTRACT

Progesterone receptor membrane component 2 (*Pgrmc2*) mRNA was detected in the immature rat ovary. By 48 h after eCG, *Pgrmc2* mRNA levels decreased by 40% and were maintained at 48 h post-hCG. Immunohistochemical studies detected PGRMC2 in oocytes and ovarian surface epithelial, interstitial, thecal, granulosa, and luteal cells. PGRMC2 was also present in spontaneously immortalized granulosa cells, localizing to the cytoplasm of interphase cells and apparently to the mitotic spindle of cells in metaphase. Interestingly, PGRMC2 levels appeared to decrease during the G₁ stage of the cell cycle. Moreover, overexpression of PGRMC2 suppressed entry into the cell cycle, possibly by binding the p58 form of cyclin dependent kinase 11b. Conversely, *Pgrmc2* small interfering RNA (siRNA) treatment increased the percentage of cells in G₁ and M stage but did not increase the number of cells, which was likely due to an increase in apoptosis. Depleting PGRMC2 did not inhibit cellular ³H-progesterone binding, but attenuated the ability of progesterone to suppress mitosis and apoptosis. Taken together these studies suggest that PGRMC2 affects granulosa cell mitosis by acting at two specific stages of the cell cycle. First, PGRMC2 regulates the progression from the G₀ into the G₁ stage of the cell cycle. Second, PGRMC2 appears to localize to the mitotic spindle, where it likely promotes the final stages of mitosis. Finally, siRNA knockdown studies indicate that PGRMC2 is required for progesterone to slow the rate of granulosa cell mitosis and apoptosis. These findings support a role for PGRMC2 in ovarian follicle development.

apoptosis, granulosa cells, mitosis, PGRMC1, PGRMC2, progesterone

INTRODUCTION

Progesterone (P4) slows the rate at which granulosa cells and immortalized cells derived from granulosa cells, that is, spontaneously immortalized granulosa cells (SIGCs), undergo

mitosis and apoptosis in vitro [1–9]. However, the classic nuclear progesterone receptor (PGR) does not mediate P4's actions because granulosa cells of growing follicles and SIGCs do not express PGR [10–13]. Rather, P4's actions in these cells are mediated through PGR membrane component 1 (PGRMC1) [14, 15] as demonstrated by genetic manipulation of PGRMC1 levels in cultured cells [9, 14–17].

While PGRMC1 is the first member of the membrane-associated PGR family to be identified [18], this family also includes other family members such as PGRMC2 [18]. The amino acid sequences of these two proteins are very similar with the major differences being observed distal to the transmembrane region (reviewed by Cahill [19]). Although there are numerous publications on PGRMC1, to date there are only two published studies on the expression of PGRMC2 in the mammalian ovary and these are microarray-based. For example, microarray and subsequent PCR analysis reveals that *Pgrmc2* is expressed at the time of follicle assembly in the neonatal rat ovary [20]. The other paper reports that granulosa cell *Pgrmc2* mRNA levels are elevated in women with diminished ovarian reserve [21]. Interestingly, these women develop fewer follicles in response to gonadotropin treatment [21]. Taken together, these two studies imply that PGRMC2 plays a role in both the formation and development of ovarian follicle. Given the limited amount of data regarding the expression and function of PGRMC2 in the ovary, the present study was designed to determine the expression of *Pgrmc2* in the gonadotropin-primed immature rat ovary, freshly isolated rat granulosa cells, and SIGCs. Subsequent studies were then undertaken to determine whether PGRMC2 1) influences the rate of SIGC mitosis, 2) binds ³H-P4, and/or 3) mediates P4's actions on mitosis and apoptosis.

MATERIALS AND METHODS

All the reagents were purchased from Sigma Chemical Co. unless specified otherwise. Additional information regarding the antibodies used in these studies is presented in Supplemental Table S1 (Supplemental Data are available online at www.biolreprod.org).

Collection and Processing of Immature Rat Ovaries after Gonadotropin Treatment

Immature female Sprague-Dawley rats between 22 to 25 days of age were obtained from the colony at Washington State University. A group of four immature control rats was treated i.p. with saline for 48 h and then euthanized by carbon dioxide exposure and cervical dislocation. A second group of nine rats was injected i.p. with 5 international units equine chorionic gonadotropin (eCG) (EMD Millipore). Four of these rats were euthanized and the ovaries collected 48 h later. The remaining five rats were injected i.p. with 5 international units human chorionic gonadotropin (hCG) and 48 h later were euthanized and the ovaries prepared for PGRMC2 analysis. This protocol was approved by the Institutional Animal Care and Use Committee at Washington

¹Supported by NIH grant R01 HD 052740 awarded to J.J.P.; NIH grant R21RR030264 awarded to J.J.P. and J.K.P.; and R21 HD066297 awarded to J.K.P.

²Correspondence: John J. Peluso, Department of Cell Biology, University of CT Health Center, Farmington, CT, 06030. E-mail: peluso@nso2.uhc.edu

³Permanent address: Boston IVF at The Women's Hospital, Reproductive Endocrinology, 4199 Gateway Blvd., Suite 2600, Newburgh, IN 47630. E-mail: Daniel.Griffin@deaconess.com

Received: 9 January 2014.

First decision: 29 January 2014.

Accepted: 23 June 2014.

© 2014 by the Society for the Study of Reproduction, Inc.

eISSN: 1529-7268 <http://www.biolreprod.org>

ISSN: 0006-3363

State University. For all the treatment groups, one ovary was fixed in 4% paraformaldehyde, paraffin embedded, and processed for immunohistochemical localization of PGRMC2 as described below. Total RNA was isolated from the remaining ovary from each rat using Trizol (Life Technologies) and stored at -80°C until analyzed for *Pgrmc2* mRNA.

Granulosa Cell and SIGC Culture

For the granulosa cell culture studies, immature female Sprague-Dawley rats (21 days of age) were obtained from Charles River Laboratory. At 22–25 days of age, rats were euthanized by carbon dioxide exposure followed by cervical dislocation. The ovaries were removed, trimmed of fat, and the follicles punctured with a 26 g needle to release the granulosa cells [14]. The granulosa cells were isolated and plated at $4 \times 10^5/\text{ml}$ in a 35 mm² dish (Becton Dickinson) with cover glass on the bottom. This protocol was approved by the University of CT Health Center Institutional Animal Care and Use Committee.

SIGCs, which were derived from granulosa cells of rat preovulatory follicles [22], were maintained in culture as previously described [14, 15]. Unless otherwise stated, 4×10^5 cells were placed in 35 mm² dishes with or without a cover glass in 2 ml of DMEM/F12 with 5% fetal bovine serum (FBS). In the experiments involving the effects of 1 μM P4, cells were cultured in DMEM/F12 supplemented with 5% steroid-free FBS (Hyclone).

Immunochemical Localization of PGRMC2

To localize PGRMC2 within the rat ovary, paraffin-embedded ovaries were sectioned at 5 μm . The sections were deparaffinized, and endogenous peroxidase activity was quenched by exposure to hydrogen peroxide. Then the sections were boiled for 10 min in 10 mM sodium citrate buffer (pH 6.0) and subsequently incubated overnight at 4°C with combined primary (1:100, PGRMC2 clone 3C11) and secondary (1:2000; Life Technologies) antibodies, which were previously incubated for 2 h at 37°C in blocking solution containing normal mouse serum to eliminate nonspecific binding. Sections were then washed in PBS, incubated in horseradish peroxidase-conjugated streptavidin for 45 min at room temperature (Vector Laboratories), washed in PBS, and incubated with 3,3'-diaminobenzidine substrate. Sections were then methyl-green counterstained. PGRMC2 was revealed as a brown precipitate. As a negative control, ovarian sections were incubated using the same protocol but with nonimmune immunoglobulin G (IgG) replacing the primary antibody.

For immunocytochemical localization studies, granulosa cells and SIGCs that were plated on cover glass were fixed with 4% paraformaldehyde, washed in PBS, permeabilized with 0.1% Triton X-100, and incubated in 5% normal goat serum for 1 h at room temperature. The cells were then incubated overnight at 4°C with a mouse monoclonal anti-PGRMC2 antibody (Clone 3C11, 1:200 in 0.1% bovine serum albumin/PBS). Negative controls were incubated without the primary antibody. Cells were then washed with PBS and incubated for 1 h with goat anti-mouse antibody tagged with either Alexa Fluor 546 (red fluorescence) or Alexa Fluor 350 (blue fluorescence) (Molecular Probes) to detect the primary PGRMC2 antibody. The use of the secondary antibody to detect PGRMC2 was dependent on the experimental objective.

Changes in PGRMC2 Expression During the Cell Cycle

To determine if PGRMC2 expression was cell cycle dependent, SIGCs were infected with fluorescence ubiquitination cell cycle indicator (FUCCI) (P36237; Life Technologies). Briefly, SIGCs were infected with FUCCI (20 viral particles per cell) and cultured at 37°C for 24 h. FUCCI utilizes a baculovirus (BacMan 2.0) to infect cells with DNA that encodes the ubiquitination domains of either the geminin-green fluorescent protein (GFP) fusion protein or cytolethal distending toxins (cdt)-red fluorescent protein (RFP) fusion protein [23]. To assess the efficiency of the baculovirus infection, SIGCs were separately infected with a baculovirus (BacMan 2.0) that encodes an actin-GFP fusion protein (C10582; Life Technologies).

Note that cdt and geminin are expressed in the G_1 and G_2 stages, respectively, while both are expressed in the S stage of the cycle [23]. Twenty-four hours after infection, the cells were fixed and stained for PGRMC2 as described above using an Alexa350 (blue) secondary antibody. Using this protocol, nonfluorescent cells with interphase nuclei were considered to be in the G_0 stage, red fluorescent cells were in the G_1 stage, and green fluorescent cells were in the G_2 stage. S stage cells were observed as fluorescing yellow after merging the green and red fluorescent signals. The fluorescent intensity of the blue signal was used to estimate the level of PGRMC2. The relationship between PGRMC2 expression and each stage of the cell cycle was determined by fluorescent microscopy.

Genetic Manipulation of *Pgrmc1* and/or *Pgrmc2* Levels

To assess the effect of PGRMC2 on entry into the cell cycle, SIGCs were simultaneously infected with the baculovirus that encodes the cdt-RFP fusion protein and transfected with either the GFP empty vector (control) or GFP-PGRMC2 expression construct using Lipofectamine 2000 as previously described [17]. The GFP expression construct, which encodes human *Pgrmc2*, was provided by Dr. Martin Wehling (University of Heidelberg at Mannheim) [24]. Its identity was confirmed by DNA sequencing. After infection/transfection the cells were cultured in 5% steroid-free FBS in DMEM overnight. After 24 h of culture, cultures were examined by fluorescent microscopy, and for each experiment, 200 cells that expressed the GFP protein were identified. Then these GFP-expressing cells were observed under the RFP filter set to determine if they were in the G_1/S stage of the cell cycle. The percentage of transfected cells in the G_1/S stage was calculated for each treatment group.

To determine the effect of depleting PGRMC2, SIGCs were cultured for 24 h and then transfected using Lipofectamine 2000 with *Pgrmc1* or *Pgrmc2* siRNA (small interfering RNA). The siRNA sequences for rat *Pgrmc1* and *Pgrmc2* siRNAs were CCUGGUAUUUGGCAGUUGGtt (253165; Life Technologies) and GGAAAUGCAGUUUAAAGAAtt (s168258; Life Technologies), respectively. As a control, a scramble siRNA control (AM4611; Life Technologies) was used. Twenty-four hours after transfection, the cells from one 35 mm² dish were harvested, replated into two 35 mm² dishes, and cultured with DMEM/F12 supplemented with 5% FBS for an additional 24 h. The cultures were then used either to 1) measure *Pgrmc1* and *Pgrmc2* mRNA levels by real-time PCR, 2) monitor PGRMC2 by immunocytochemistry, or 3) assess the percentage of cells at each stage of the cell cycle using the FUCCI probe.

Pgrmc1 and *Pgrmc2* mRNA Measurements by Real-Time PCR

RNA was isolated from the SIGCs using RNeasy Plus Mini-Kit (Qiagen) per the manufacturer's instructions and converted to cDNA [17]. A 20 μl reaction tube was made by adding SsoFast Probes Supermix (Bio-Rad Laboratories), 1 ng of the cDNA, forward primers (*Pgrmc1* 5' TGAGAG CAATATACAGGACAGGAA 3' or *Pgrmc2* 5' GCTACTCAGTGTGCAGA TCTCT 3'), reverse primers (*Pgrmc1* 5' ACCCAGCTAGTGCCATGTAGTG 3' or *Pgrmc2* 5' CCAGGGCTCTCCCTTAACAC 3'), and probes (*Pgrmc1* 5' FAM-TGCGCTTTTCAAAGCTTCCACTGA-BHQ-1 3' or *Pgrmc2* 5' FAM-AAGGACAAGGGATCCTGTTTCCACA-BHQ-1 3'). Actin served as a control and was detected using forward primer (5'd CGGTGAGTGCAT CACTATCG 3'), reverse primer (5'd TTCCATACCCAGGAAGGAAG 3'), and probe (5'd CAL Fluor Gold 540-AATGAGCGGTTCCGATGCCC-BHQ-1 3'). The real-time PCR reaction was run in the CFX96 real-time PCR system. The cycling steps for enzyme activation were 30 sec at 95°C , denaturation for 5 sec at 95°C , and annealing/extension at 60°C for 1–10 sec; 40 cycles were conducted. Gene expression was evaluated using Bio-Rad CFX96 software. *Pgrmc1* and *Pgrmc2* levels were normalized to actin and expressed as a percentage of the scramble treatment group.

For *Pgrmc2* expression analysis in rat ovaries, total RNA was first treated with DNase I to eliminate contaminating DNA and then purified using RNeasy Plus Mini-Kit (Qiagen) per the manufacturer's instructions. RNA was next converted to cDNA using Superscript II (Life Technologies). A 20 μl reaction was set up for each sample in which 1.5 ng cDNA, Syber Green PCR Master Mix, *Pgrmc2* forward primer (5'd TCGAGAGTGGGAAATGCAGT 3'), and *Pgrmc2* reverse primer (5'd GCTCTTCCCCTGGCTTTAGG 3') were included. The ribosomal protein *Rpl13a* was used as an internal control (5'd AAAGGTGGTGGTTGTACGCT 3' and 5' AGACGGGTTGGTTCATCC 3'). The real-time PCR reaction was run in the CFX96 real-time PCR system. The cycling steps for enzyme activation were 10 min at 95°C , denaturation for 15 sec at 95°C , and annealing/extension at 60°C for 1 min; 40 cycles were conducted. Gene expression was evaluated using Bio-Rad CFX96 software where *Pgrmc2* levels were normalized to *Rpl13a* and expressed as a percentage of the nongonadotropin-treated control.

Identification of Cyclin Dependent Kinase 11b as a PGRMC2 Binding Partner

To gain insight into PGRMC2's mode of action, SIGCs were transfected with GFP-PGRMC2. Twenty-four hours later, GFP-PGRMC2 and associated proteins were isolated as described in our previously published protocol [15]. Briefly, the transfected SIGCs were lysed in cold RIPA buffer and the supernatant collected. The GFP-PGRMC2 fusion protein and associated proteins were isolated using the anti-GFP microbeads and the protocol and reagents provided by Miltenyi Biotec. The isolate was then sent to Yale

University Keck Foundation for Biotechnology Mass Spectrometry and Protein Identification facility. The PGRMC2-associated proteins were identified by liquid chromatography-mass spectrometry/mass spectrometry after enzymatic (trypsin) digestion. This analysis revealed a potential interaction with the cyclin-dependent kinase, CDK11b. The presence of GFP-PGRMC2 in the isolate was confirmed by Western blot analysis using the GFP antibody (1:1000; Cell Signaling) or the PGRMC2 antibody (1:200).

The interaction between GFP-PGRMC2 and CDK11b was confirmed using two approaches. First, additional experiments were conducted in which GFP-PGRMC2 and associated proteins were isolated using anti-GFP microbeads as described above. The isolate was used in a Western blot analysis that was probed with a CDK11b antibody (sc-928; Santa Cruz Biotechnology). Similar experiments were conducted in which GFP-empty vector was transfected and the GFP isolate run on Western blot and probed with CDK11b antibody.

The second approach involved colocalization and an in situ proximity ligation assay (PLA) that were conducted as described in our previous publication [6]. The colocalization of PGRMC2 and CDK11b was conducted using the PGRMC2 and CDK11b antibodies and the immunocytochemical protocol outlined previously. Because colocalization is not sufficient to demonstrate a protein-protein interaction, an in situ PLA (Duolink II; OLINK Bioscience) was conducted according to the manufacturer's instructions. In this assay, the same primary antibodies to PGRMC2 and CDK11b were used, but the secondary antibodies were labeled with complementary oligonucleotide strands that generate a signal (a red fluorescent spot) only when the two proteins are bound to each other (<http://www.olink.com/>).

³H-Progesterone Binding to Intact SIGCs

For these studies SIGCs were plated in 96-well culture plates (4×10^4 /well) and transfected with either scramble, *Pgrmc1*, or *Pgrmc2* siRNA as previously described [17, 25] with the exception that the cultures were not replated after 24 h of culture. After 48 h of culture, ³H-P4 binding studies were conducted, and the amount of ³H-P4 specifically bound to SIGCs was determined as previously described [13, 26]. Specific ³H-P4 binding was expressed as a percentage of the scramble control. The binding experiments were repeated four times and values are means \pm SEM.

Assessment of Cell Proliferation and Apoptosis

SIGCs were plated and transfected with *Pgrmc2* siRNA as described above with the exception that after the initial 24 h culture period the cells were replated in 35 mm² dishes in which the bottom plate was scored with a diamond pen to identify four quadrants. Two hours after replating, the culture medium was removed and the dishes were washed gently with DMEM/F12 to remove any cells that were not firmly attached. The culture medium was then replaced with medium with or without supplemental P4 (1 μ M) and pictures taken of each quadrant. After 22 h of culture, pictures were taken of the same quadrants. The number of cells in each quadrant at 2 and 24 h of culture was counted and used to calculate fold increase in cell number. Cells were also fixed and stained with 4',6-diamidino-2-phenylindole (DAPI) in order to calculate the percentage of apoptotic cells. A cell was considered apoptotic if its nucleus was condensed and/or fragmented [17].

Statistical Analysis

All the experiments were replicated at least three times unless stated otherwise. All the animals were assigned to treatment groups randomly. Values from each experiment were pooled to generate a mean \pm SEM. Differences between treatment groups were assessed by Student *t* test if only the means of two groups were compared or by an ANOVA followed by the Fisher LSD post hoc test if more than two treatment groups were compared. Regardless of the analysis, $P \leq 0.05$ was considered to be significantly different.

RESULTS

Ovarian levels of *Pgrmc2* mRNA were highest prior to gonadotropin treatment. By 48 h after eCG, the ovarian levels of *Pgrmc2* mRNA decreased by $\approx 40\%$ and were maintained at this level after hCG treatment (Fig. 1A). Immunohistochemical studies revealed that PGRMC2 was present in all the cell types within the ovary with the most pronounced staining observed within the corpora lutea (Fig. 1, B and E) and interstitial tissue after eCG-hCG treatment (Fig. 1B). Intense staining for PGRMC2 was also present in the surface epithelial cells of ovaries prior to and after gonadotropin treatment (Fig. 1C).

Staining was also evident in the thecal cells, granulosa cells, and oocytes of preantral (Fig. 1C) and antral follicles (Fig. 1D). Staining for PGRMC2 was also observed in luteal cells present after eCG-hCG treatment (Fig. 1E). Note that the brown staining, which revealed PGRMC2, was not observed in luteal cells when the PGRMC2 antibody was replaced by nonimmune IgG in the staining protocol, demonstrating the specificity of the immunohistochemical detection of PGRMC2 (Fig. 1F). Similarly when IgG replaced the PGRMC2 antibody, brown staining was not observed in thecal, granulosa, surface epithelial and interstitial cells, or oocytes (Supplemental Fig. S1).

Immunocytochemical staining also detected PGRMC2 in both freshly isolated granulosa cells from nongonadotropin-primed immature rat ovaries (Fig. 2A) and SIGCs (Fig. 2B). The PGRMC2 immunocytochemical protocol was specific because only minimal fluorescence was detected in the absence of the PGRMC2 antibody (Fig. 2C) or after PGRMC2 siRNA treatment (compare Fig. 7C with 7B).

These studies demonstrated that PGRMC2 predominately localized to the cytoplasm. In metaphase, PGRMC2's localization was consistent with it being associated with the mitotic spindle (Fig. 2B inset). For interphase cells, the intensity of PGRMC2 staining was variable, suggesting the possibility that PGRMC2 expression was cell cycle dependent.

To test this possibility, we opted to infect cells with the FUCCI because it can precisely identify cells in G₁ unlike DNA-based fluorescence-activated cell sorting (FACS) analysis, which groups G₀/G₁ stage cells together. Although the use of FUCCI to monitor changes in the cell cycle is relatively new, its application has been well documented (See Supplemental Data on FUCCI). However, one limitation of using FUCCI is that FUCCI-infected cells in the G₀ stage do not fluoresce, which is a limitation only if the infection efficiency is low. In order to estimate infection efficiency, cells were infected using baculovirus (BacMan 2.0) that encodes actin-GFP fusion protein. Twenty-four hours after infection with the baculovirus encoding actin-GFP, an average of 86% of the cells fluoresced green, indicating that they were expressing the actin-GFP fusion protein (Supplemental Fig. S2). This infection rate is in line with the estimated 90% infection rate provided by the manufacturer. Given that baculovirus (BacMan 2.0) is used to infect cells with the FUCCI probe and therefore has the same infection rate as actin-GFP, it is estimated that $\leq 14\%$ of the SIGCs would not be infected with the FUCCI probe. These noninfected cells would be distributed proportionately to cells in each stage of the cell cycle; thus, the error due to infection efficiency would appear to be relatively minor.

Given that this limitation would not significantly impair the ability to determine the stage of the cell cycle, SIGCs were infected with FUCCI; the DNA stained with Hoechst 33342 and the percent of cells in each stage of the cell cycle estimated by FACS using standard DNA-based or FUCCI-based analyses. As can be seen in Supplemental Figure S3A, DNA-based FACS analysis does not distinguish cells in G₁ from those in G₀. However, FACS analysis of FUCCI-infected cells readily identifies cells in each stage of the cell cycle (Supplemental Fig. S3B), regardless of whether FUCCI-expressing cells are monitored by FACS or by fluorescent microscopy (Supplemental Fig. S3C).

Fluorescent microscopic examination of FUCCI-infected cells stained with DAPI can also be used to identify cells in each stage of the cell cycle. As with FACS, fluorescent microscopic detection of SIGCs in different stages of the cell

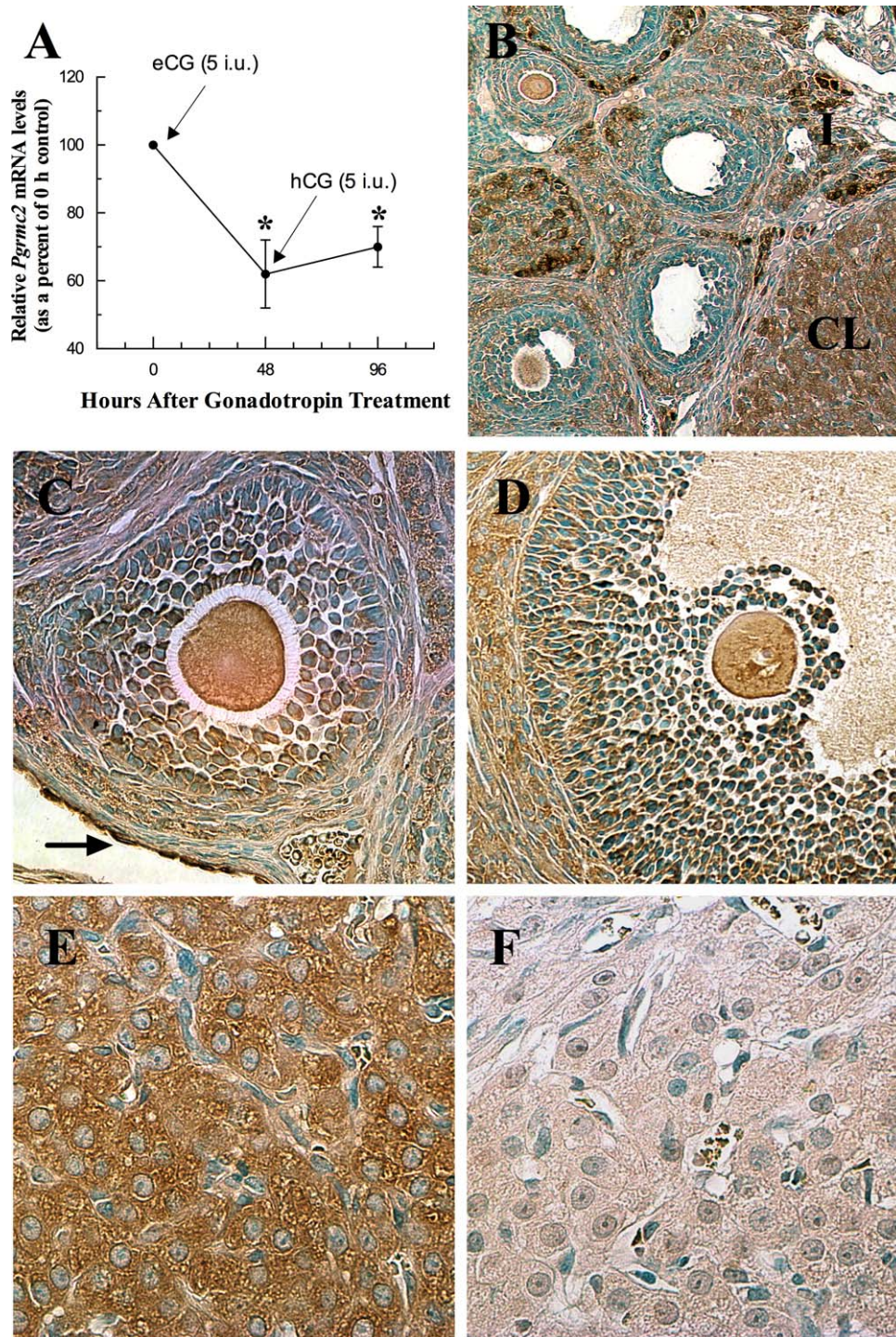


FIG. 1. The expression of PGRMC2 in the gonadotropin-primed immature rat ovary. **A**) The effect of sequential injections of eCG and hCG on the relative *Pgrmc2* mRNA levels is shown. Values are expressed as the mean \pm SEM, and * indicates values that are significantly less than the 0 h control ($P < 0.05$). **B**) A low-power image of an eCG-hCG treated ovary stained for PGRMC2. The most intense brown staining, which indicates the presence of PGRMC2, was observed in the corpus luteum (CL) and interstitium (I), but thecal cells, granulosa cells, and oocytes also stained for PGRMC2. **C**) A preantral follicle from an immature rat ovary. PGRMC2 staining was detected in the oocyte as well as granulosa and thecal cells of this follicle. The ovarian surface epithelial cells were also intensely stained for PGRMC2 (arrow). A large antral follicle of an eCG-primed rat ovary is shown in **D**, which shows PGRMC2 staining in the oocyte, granulosa, and thecal cells. **E**) A higher power image of luteal cells taken from an eCG-hCG treated immature rat. Note that PGRMC2 was localized to the cytoplasm. **F**) A higher power image of luteal cells taken from an eCG-hCG treated immature rat that serves as a negative control because the PGRMC2 antibody was replaced with nonimmune IgG. Images taken at magnifications of $\times 100$ (**B**), $\times 200$ (**C**, **D**), and $\times 400$ (**E**, **F**).

cycle is based on their fluorescence (i.e., G_1 fluoresce red; S fluoresce yellow; G_2 fluoresce green; and G_0 and M fluoresce blue) (Fig. 3A). Note that the percent of cells in each stage of the cell cycle was similar regardless of whether the analysis

was conducted using FACS or fluorescent microscope (Supplemental Fig. S3C).

To define the relationship between the presence of PGRMC2 and the stage of the cell cycle, cells were infected

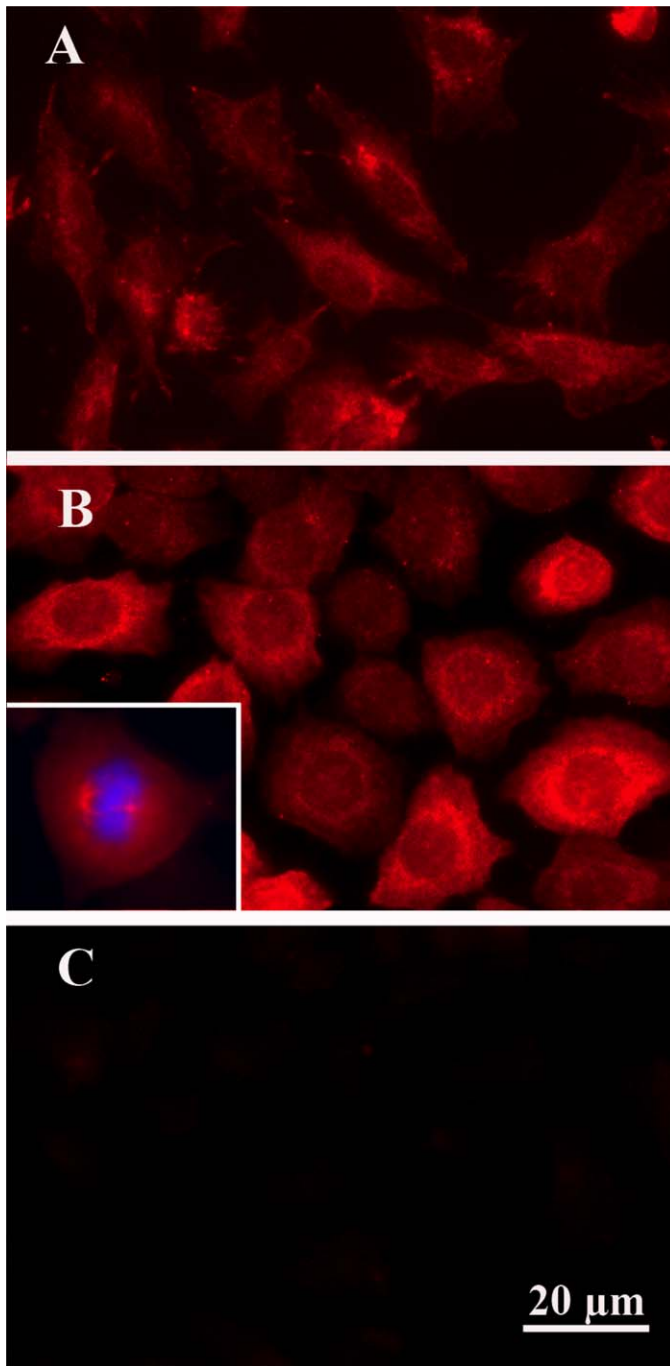


FIG. 2. The expression of PGRMC2 in freshly isolated granulosa cells obtained from an immature rat ovary (A) and spontaneously immortalized granulosa cells (SIGCs) (B). PGRMC2 was detected by immunofluorescence (red fluorescence). The inset in B shows a DAPI-stained cell (blue fluorescence) in metaphase with the chromosomes arranged on a metaphase plate. PGRMC2 surrounds the chromosomes, consistent with PGRMC2 localizing to the mitotic spindle. Note that red fluorescence was not observed in the cells that served as negative controls (C).

with FUCCI and then stained for PGRMC2 using the Alexa Fluor 350-labeled secondary antibody (blue fluorescence), but not with DAPI, and examined under the fluorescent microscope. This analysis revealed that cells in the G_1 stage of the cell cycle (Fig. 3B) appeared to express less PGRMC2 than those cells in G_0 (Fig. 3b). Note that cells in S or G_2 had the same level of PGRMC2 expression as those cells in G_0 (compare Fig. 3C with 3c). This cell cycle-dependent change in

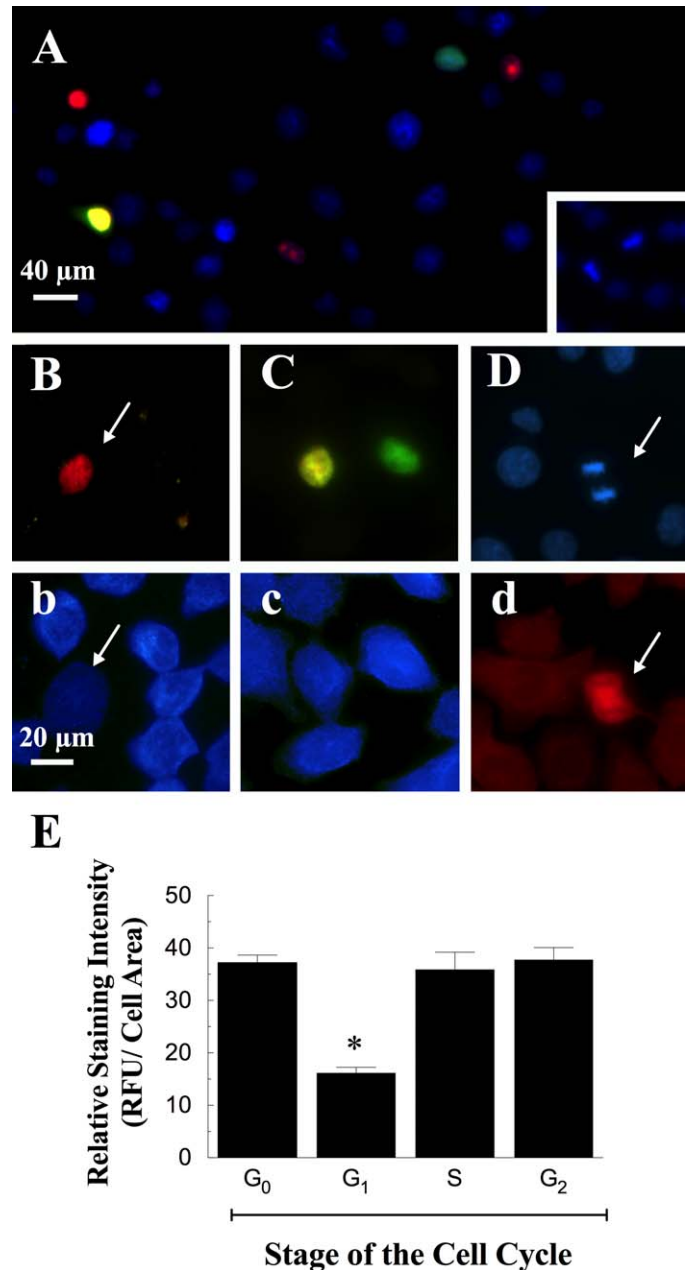


FIG. 3. The relationship between PGRMC2 expression and the stage of the cell cycle as assessed by microscopic analysis of FUCCI-infected SIGCs. A) SIGCs were infected with the FUCCI, fixed, and then stained with DAPI. Cells that fluoresced blue were considered to be in either G_0 or undergoing mitosis (inset), depending on its nuclear structure. Red fluorescent cells were in G_1 stage, and green fluorescent cells were G_2 stage. S-stage cells were observed as fluorescing yellow after merging the green and red fluorescent images. B, C) The relationship between PGRMC2 expression and the cell cycle as judged by FUCCI. In B, a cell in the G_1 -stage (red) is detected. There are other cells in this field that are not detected because the cells were not stained with DAPI. In b, PGRMC2 staining is shown (blue) for the same field of cells as shown in B with the G_1 stage cell marked by an arrow. C) Shows cells in either the S-stage (yellow) or G_2 -stage (green) of the cell cycle. In c, PGRMC2 staining is shown (blue) for the same field of cells as shown in C. D) DAPI-stained cells with one cell in anaphase (arrow), while d shows PGRMC2 staining consistent with PGRMC2 being associated with the mitotic spindle (arrow). In E, semiquantitative estimates of PGRMC2 expression are shown as a function of the stage of the cell cycle. These estimates are expressed as relative fluorescent units (RFU)/cell area based on fluorescent intensity values obtained from the iVision Image Acquisition and Analysis Software (BioVision Technologies). Values are expressed as the mean \pm SEM. The * indicates a value that is significantly different than all the other groups ($P < 0.05$).

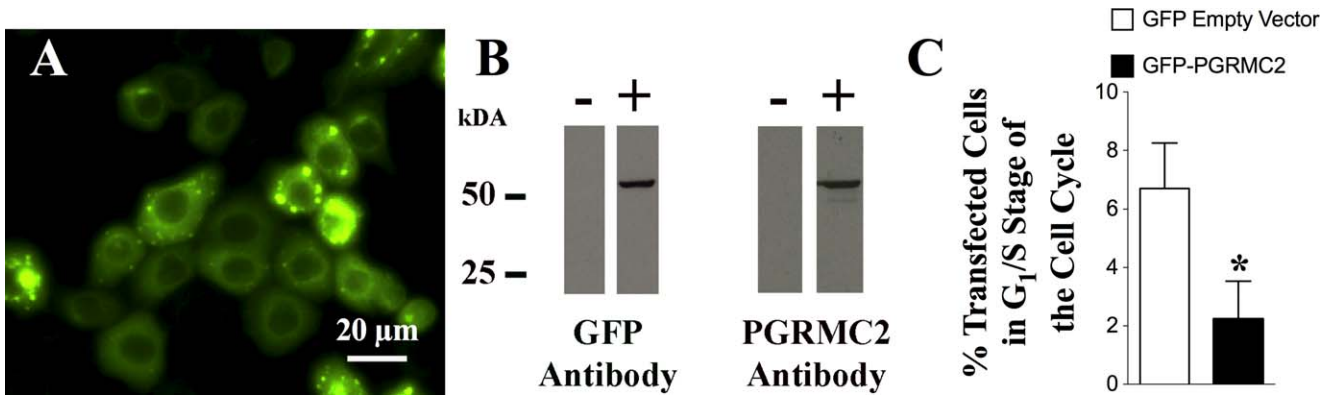


FIG. 4. The effect of overexpression of GFP-PGRMC2 on entry into the cell cycle. **A**) The cellular localization of the GFP-PGRMC2 fusion protein. The Western blots of the GFP isolate is shown in **B**, which demonstrates that the appropriate-sized GFP-PGRMC2 fusion protein (27 kDa for GFP and 24 kDa for PGRMC2) is detected by both a GFP and PGRMC2 antibody. In **B**, lanes marked with a minus sign (-) indicate a negative control in which the primary antibody was omitted. Lanes marked with a plus sign (+) indicate the Western blot protocol include the primary antibody. For details, see the *Materials and Methods* section. **C**) Shows the effect of GFP-PGRMC2 overexpression on the percentage of cells in the G₁/S-stage of the cell cycle as judged by FUCCI staining. Values are expressed as the mean ± SEM. The * indicates a value is significantly less than the empty vector control ($P < 0.05$).

PGRMC2 expression was also reflected in the semiquantitative measurements of the fluorescent intensity of PGRMC2 staining (Fig. 3E).

To assess the localization of PGRMC2 in cells during mitosis, PGRMC2 was detected using a secondary antibody labeled with Alexa Fluor 546 (red fluorescence) and the chromosomes stained with DAPI (blue fluorescence). This analysis revealed that PGRMC2 appeared to localize to the mitotic spindle at all stages of mitosis, including metaphase (Fig. 2B inset) and anaphase (compare Fig. 3D with 3d).

The transient suppression of PGRMC2 at the G₁ stage implied that the levels of PGRMC2 decrease in order to allow cells to enter the cell cycle. To test this hypothesis, PGRMC2 levels were increased by transfecting the cells with a GFP-PGRMC2 expression vector. Like endogenous PGRMC2, GFP-PGRMC2 was localized predominately in the cytoplasm (Fig. 4A) and was detected by Western blots that used isolate obtained after partial purification of the GFP-PGRMC2 fusion protein (Fig. 4B). This analysis detected GFP-PGRMC2 as a single ≈55 kDa band using either the GFP antibody or the

PGRMC2 antibody (Fig. 4B). As seen in Figure 4C, overexpression of PGRMC2 reduced the percentage of cells that entered the G₁/S stage of the cell cycle compared to the GFP empty vector control.

In an attempt to gain insight into the mechanism through which GFP-PGRMC2 suppressed entry into the cell cycle, proteins that interacted with GFP-PGRMC2 were identified using a mass spectrometric approach. This analysis revealed that CDK11b interacted with GFP-PGRMC2. CDK11b exists as an inactive or active form, detected as 110 and 58 kDa proteins, respectively [27]. Western blots using whole cell lysate detected the 58 kDa form (Fig. 5A), but the 110 kDa form was occasionally detected depending on the duration of imaging. To confirm that CDK11b interacts with GFP-PGRMC2, GFP-PGRMC2 was transfected into cells and partially purified, and the purified GFP-PGRMC2 preparation used in a Western blot analysis. Probing this Western blot with the CDK11b antibody detected the 58 kDa form (Fig. 5B). Note that in this experiment, staining with the GFP antibody not only detected the ≈55 kDa GFP-PGRMC2 fusion protein

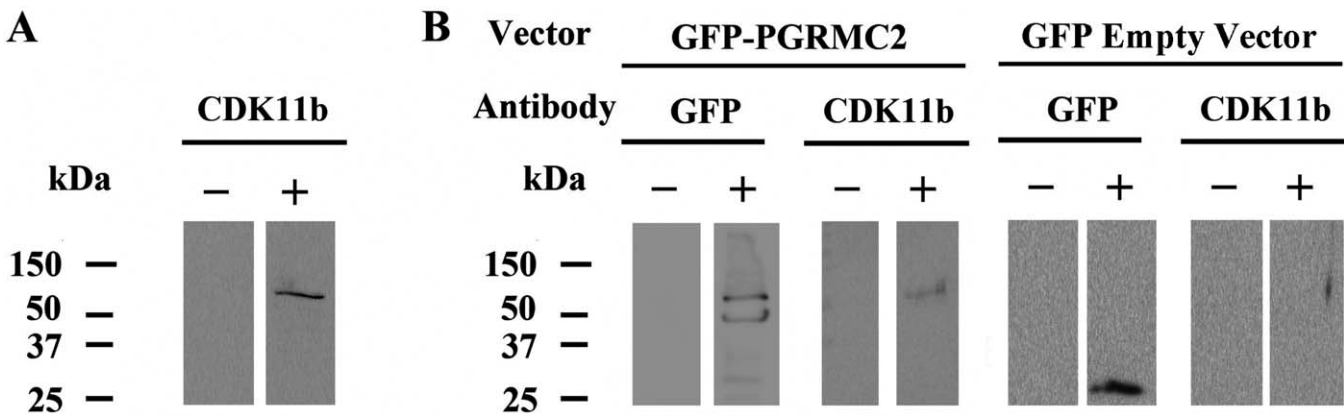


FIG. 5. The expression of CDK11b (**A**) and its interaction with GFP-PGRMC2 (**B**) as revealed by Western blot analysis. For this study, cells were transfected with GFP-PGRMC2 and a whole cell lysate was prepared. An aliquot was taken and used in the Western blot shown in **A**. The remaining lysate was used to partially purify GFP-PGRMC2 and associated proteins. Aliquots of the GFP-PGRMC2 isolate were run in Western blot protocols and probed with either the GFP antibody to detect PGRMC2 or the CDK11b antibody (**B**). **B**) The results of a similar study in which the cells were transfected with the GFP-empty vector. Note that in this study the GFP antibody detected a 27 kDa band, the expected kDa of GFP but bands were not observed when the CDK11b antibody was used. In this figure, lanes marked with a minus sign (-) indicate a negative control in which the primary antibody was omitted. Lanes marked with a plus sign (+) indicate that the Western blot protocol included the primary antibody.

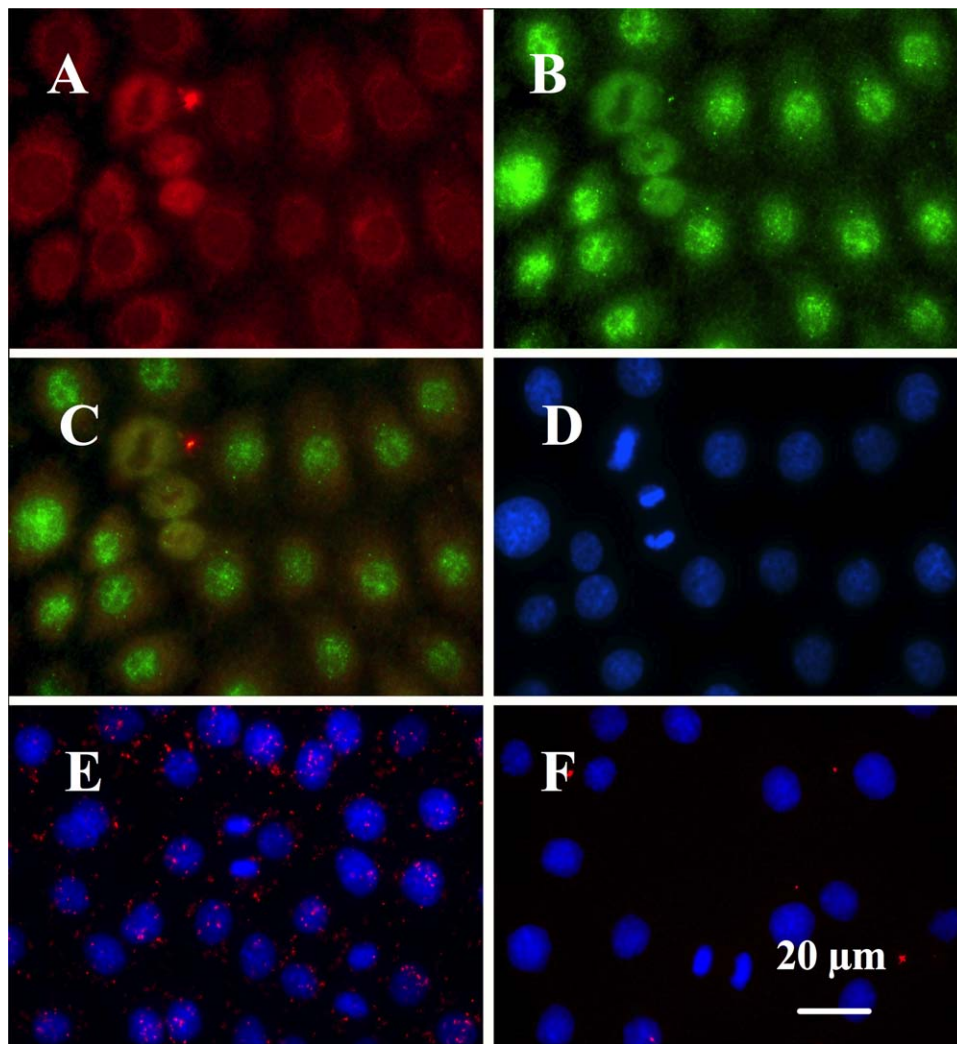


FIG. 6. Colocalization and interaction of PGRMC2 and CDK11b in SIGCs. Immunocytochemical staining for PGRMC2 and CDK11b is shown in **A** (red fluorescence) and **B** (green fluorescence), respectively, while a colocalization (i.e., merged image yellow-orange fluorescence) of these two proteins is shown in **C**. A negative control in which the primary antibody was omitted is shown in **D**. These cells were also stained with DAPI to reveal the nucleus. **D**) Merged image of a negative control in which the red, green, and blue channels are merged. Note that there is no signal in either the red or green channels, indicating the specificity of this colocalization protocol. In **E**, the interaction between PGRMC2 and CDK11b is assessed by PLA, and the interaction between these two proteins was revealed by the presence of red dots. **F**) Negative control for the PLA in which one antibody (i.e., the PGRMC2 antibody) was omitted from the PLA protocol. Note the relative absence of red dots, which indicates that the PLA was specific.

but also lower kDa forms that were assumed to be degraded forms of GFP-PGRMC2 (Fig. 5B). Importantly similar experiments in which cells were transfected with the GFP-empty vector did not detect either the 110 kDa or 58 kDa form of CDK11b (Fig. 5B), thereby confirming the specificity of this GFP-PGRMC2 pull-down assay.

The interaction between endogenous PGRMC2 and CDK11b was also supported by colocalization studies that show both proteins localizing to the cytoplasm, with CDK11b also present with the nucleus (Fig. 6A–C). That this staining was specific is demonstrated by omitting the primary antibodies (Fig. 6D). Moreover, PLA, which detects protein-protein interactions, clearly demonstrated that these two proteins interact (compare the number of red dots/cell in Fig. 6E with those in 6F, the negative control).

The role of PGRMC2 in regulating entry into the cell cycle was not only assessed by overexpression of PGRMC2 but also by depleting endogenous PGRMC2 using *Pgrmc2* siRNA. As seen in Figure 7A, *Pgrmc2* siRNA treatment reduced *Pgrmc2* mRNA levels by $\approx 90\%$ of scramble control without altering

Pgrmc1 mRNA level. That *Pgrmc2* siRNA treatment reduced PGRMC2 was confirmed by immunocytochemical analysis (compare Fig. 7B with 7C). As seen in Figure 7D, depleting PGRMC2 reduced the percentage of cells in G_0 and increased the percentage in G_1 and M stages of the cell cycle (Fig. 7D). Although the rate at which cells entered into the cell cycle was increased, the number of cells did not increase (Fig. 8B). Rather, the rate of apoptosis increased (Fig. 8C).

Finally, PGRMC2's role in mediating P4's actions was assessed by first determining if PGRMC2 affected the capacity of SIGCs to bind ^3H -P4. Data shown in Figure 8A confirmed that depleting *Pgrmc1* mRNA by $\approx 90\%$ (Fig. 7A) resulted in a corresponding decrease in the capacity of the cells to bind ^3H -P4 (Fig. 8A). However, depleting *Pgrmc2* siRNA by $\approx 90\%$ did not alter the capacity of SIGCs to bind ^3H -P4 (Fig. 8A). While depleting PGRMC2 did not reduce the capacity of SIGCs to bind ^3H -P4, the ability of P4 to suppress cell proliferation (Fig. 8B) and prevent apoptosis (Fig. 8C) was attenuated by *Pgrmc2* siRNA treatment.

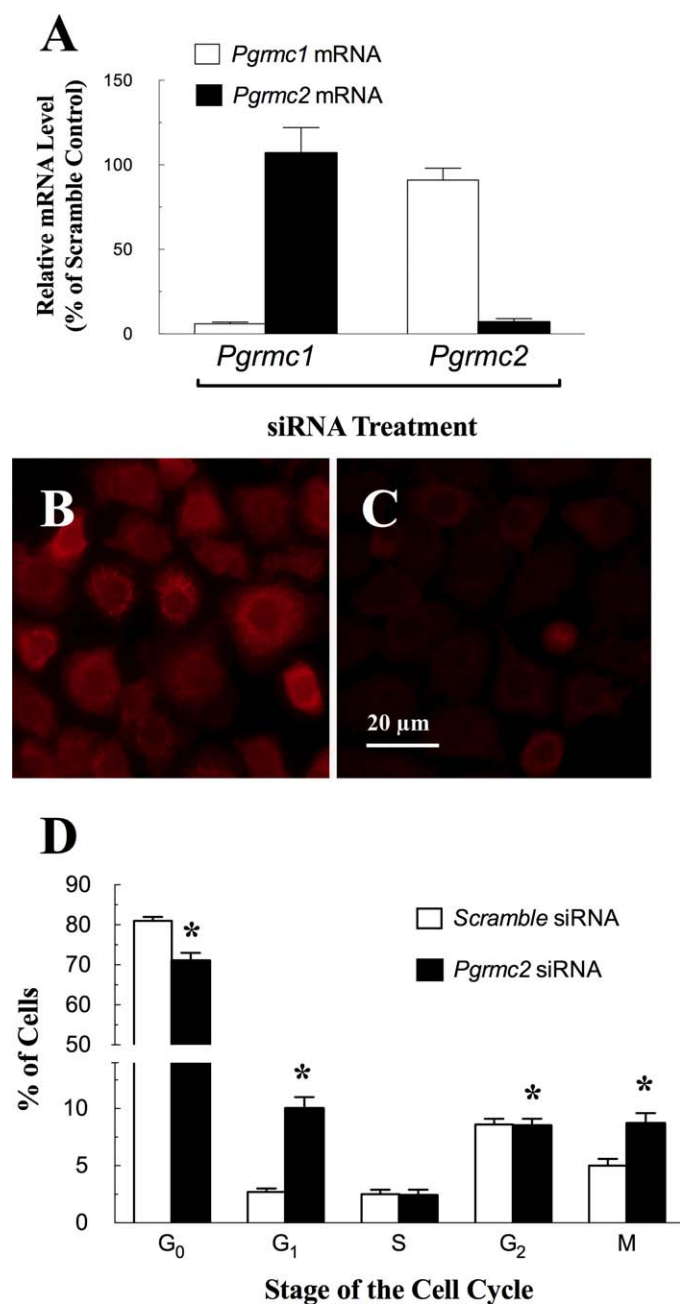


FIG. 7. The effect of *Pgrmc1* or *Pgrmc2* siRNA treatment on *Pgrmc1* and *Pgrmc2* mRNA levels (A), PGRMC2 localization assessed by immunocytochemistry after treatment with scramble siRNA (B), or *Pgrmc2* siRNA (C). The effect of scramble or *Pgrmc2* siRNA treatment on the percentage of cells in different stages of the cell cycle is shown in D. In this graph, SIGCs were classified as being in the G₀, G₁, S, G₂, or metaphase (M) stage of the cell cycle based on FUCCI probe/DAPI staining. Values are expressed as the mean \pm SEM. The * indicates a value that is significantly different from the scramble control value ($P < 0.05$).

DISCUSSION

PGRMC2 is the second member of the membrane-associated PGR family to be identified and to date has been shown to be expressed in several different cells and tissues, including mouse [28], primate [29], and bovine uterine endometrial cells [30] and oviductal epithelial cells [31] as well as placenta [32] and human granulosa/luteal cells obtained from patients undergoing in vitro fertilization [21]. In addition, PGRMC2 is expressed in peripheral blood mononuclear cells

[33], neonatal rat ovaries [20], and both ovarian [24] and breast cancers [34]. PGRMC2 mRNA is also expressed in various hypothalamic nuclei [35–37]. The present study expands this list of cell types by demonstrating that PGRMC2 is expressed in all ovarian cell types within the immature rat ovary. Moreover, its ovarian expression is regulated by gonadotropin in that its level of expression is significantly reduced by eCG. Interestingly, hCG does not alter the eCG-induced level of expression. The physiological consequences of lowering ovarian PGRMC2 levels are not known. However, PGRMC2 levels within granulosa cells may affect the capacity of follicles to develop. This précis is based on the finding that *Pgrmc2* mRNA levels in granulosa/luteal cells retrieved from in vitro fertilization patients that had a limited number of follicles develop in response to gonadotropin are elevated compared to other in vitro fertilization patients [21].

To gain insight into the function of PGRMC2, a series of studies were conducted on both freshly isolated granulosa cells and cells derived from granulosa cells (i.e., SIGCs). In these ovarian cells, PGRMC2 localizes mainly to the cytoplasm as has been shown for ovarian cancer cells [24]. Interestingly, in granulosa cells and SIGCs, the level of expression is highly variable, suggesting the possibility that PGRMC2 is expressed in a cell cycle-dependent manner.

The standard method to identify cells in specific stages of the cell cycle is to use FACS to identify the cells in different stages of the cell cycle based on their DNA content. FACS can be used on living cells, but this is not a real-time assessment because considerable time is needed to analyze the large number of cells required for this analysis. More importantly, FACS-based identification of the stages of the cell cycle is typically based on DNA content, which cannot identify cells in G₀ versus G₁ because both have similar amounts of DNA.

Because of these limitations, the present studies use the FUCCI probe to assess the stage of the cell cycle. The FUCCI probe was developed in 2008 and has been used in 37 papers, of which 22 were published in 2012–2013 (See Supplemental Data on FUCCI). Although the FUCCI probe is relatively new, the use of the FUCCI probe is the best experimental tool to test the possibility that PGRMC2 is expressed in a cell cycle-dependent manner. This precise method of monitoring the stage of the cell cycle has three major advantages. First, FUCCI detects the stage of the cell cycle in living cells with the FUCCI signal changing as an individual cell progresses through the cell cycle. The second advantage is that the FUCCI signal can be fixed, allowing PGRMC2 to be detected by immunocytochemistry. The third advantage is that the FUCCI probe clearly distinguishes cells in G₁ from those in G₀ because FUCCI does not use DNA content to make this determination.

Through the combined use of the FUCCI probe and immunocytochemistry, the present study shows that PGRMC2 levels are apparently lower in the G₁ stage than the other stages of the cell cycle. This suggests that as cells enter into G₁ they express less PGRMC2. While these expression studies imply that the suppression of PGRMC2 is required for entry into the cell cycle, it must be appreciated that the PGRMC2 expression levels were made by immunofluorescence and are semiquantitative. Unfortunately, this is the only approach available at the present time because the PGRMC2 antibody does not work effectively when used in standard Western blot protocols.

In spite of this limitation, the concept that cell cycle-dependent expression of PGRMC2 plays an essential role in regulating entry into the cell cycle is supported by two additional lines of evidence. First, expressing GFP-PGRMC2 fusion protein maintains a prolonged elevation of PGRMC2 and subsequently inhibits entry into the cell cycle. Second,

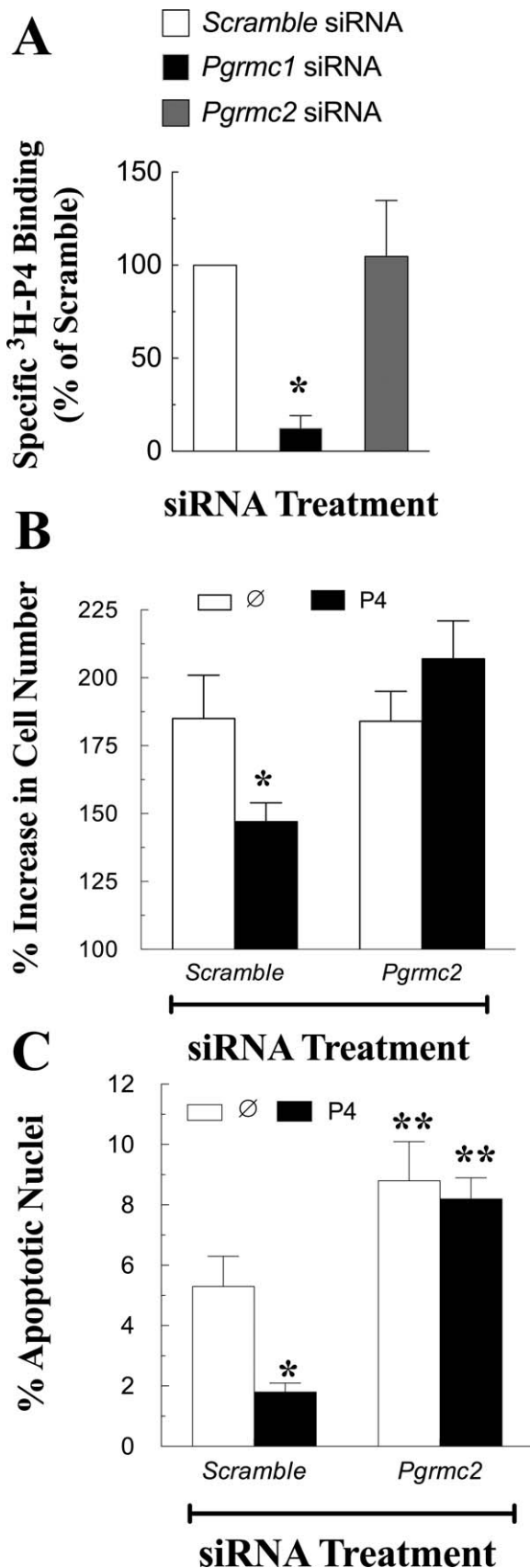


FIG. 8. The effect of *Pgrmc1* or *Pgrmc2* siRNA treatment on the capacity of SIGCs to specifically bind ³H-P4 (A). The effect of P4 on the fold increase in cell number or percentage of apoptotic nuclei for SIGCs treated with either scramble or *Pgrmc2* siRNA is shown in B and C, respectively. Values are expressed as the mean \pm SEM. The * indicates a

depleting endogenous PGRMC2 reduces the percentage of cells in the G₀ stage of the cell cycle and increases the percentage of cells in G₁ stage of the cell cycle. Thus taken together, these experimental approaches suggest that PGRMC2 regulates entry into the G₁ stage, positioning PGRMC2 to play a central role in regulating ovarian follicle development.

How PGRMC2 blocks entry into the cell cycle is unknown, but proteomic analysis indicates that GFP-PGRMC2 interacts with CDK11b, which is confirmed by independent GFP-PGRMC2 pull-down experiments shown in the present study. Moreover, colocalization and more importantly PLA studies indicate that endogenous PGRMC2 interacts with endogenous CDK11b. CDK11b is a serine/threonine kinase that is involved in cell cycle progression [38]. There are two isoforms of this kinase: a 110 (p110) and a 58 kDa (p58) form. The p58 form is active and required for normal cell cycle progression [38]. Specifically, increasing the level of the p58 form by overexpression results in early entry into the G₁ stage of the cell cycle. The p58 form of CDK11b binds cyclin D3 [39], a G₁/S stage-specific cyclin [40]. Binding cyclin D3 activates cyclin-dependent kinases [40], thereby promoting progression through the G₁/S stages of the cell cycle. It is possible then that PGRMC2 binding to the p58 form of CDK11b could inhibit CDK11b from binding cyclin D3. This would attenuate p58 CDK11b's activity and inhibit entry into the G₁ stage of the cell cycle. This concept is also consistent the present finding that PGRMC2 levels are reduced in the G₁ stage of the cell cycle, which would reduce the putative PGRMC2-CDK11b interaction, thus promoting p58 CDK11b-cyclin D3 interaction and cell cycle progression. Therefore, the proposed functional role of PGRMC2-CDK11b interaction provides a testable molecular framework that could define in part the mechanism through which PGRMC2 blocks the entry into the cell cycle.

While depleting PGRMC2 accelerates the rate at which SIGCs enter the cell cycle, it does not result in an increase in the number of cells. Rather, many PGRMC2-deplete SIGCs accumulate in metaphase, apparently failing to complete the final stages of mitosis. Moreover, it is likely that these cells undergo apoptosis. The reason for this likely relates to PGRMC2 localizing to the mitotic spindle. However, a definitive role for PGRMC2 during metaphase remains to be determined.

The present study also confirms that P4 suppresses granulosa cell proliferation and apoptosis [2, 3, 9]. Because P4's action is mediated at least in part through PGRMC1 [41], it is possible that P4 also acts through PGRMC2 to suppress mitosis and apoptosis, given PGRMC2's similarity to PGRMC1 [18, 19]. There are several mechanisms through which PGRMC2 could mediate P4's effects. The mostly likely mechanism is that PGRMC2 binds P4 and subsequently activates a signal cascade that inhibits mitosis and apoptosis. However, this does not appear to be the case because depleting PGRMC2 does not affect the capacity of SIGCs to bind ³H-P4. In contrast, depleting PGRMC1 essentially eliminates ³H-P4 binding to SIGCs. This finding is consistent with the observation that partially purified PGRMC1 binds ³H-P4, confirming that PGRMC1 is essential for P4 to bind SIGCs [15]. However, PGRMC1 may not directly bind ³H-P4 but rather function through its interaction with PAQR7, also referred to as membrane progesterin receptor alpha [42].

← value that are significantly less than scramble control value ($P < 0.05$), while ** indicates a value that is significantly greater than the scramble control value ($P < 0.05$).

Although PGRMC2 does not appear to bind P4, it is involved in mediating P4's capacity to suppress cell mitosis and apoptosis. This conclusion is based on the fact that in the relative absence of PGRMC2, P4 neither inhibits mitosis nor apoptosis even though P4 binds to PGRMC2-deplete SIGCs. These observations indicate that PGRMC2 is an essential component of the P4-signaling pathway and plays a role subsequent to P4 binding.

In summary, the present study demonstrates that PGRMC2 is expressed in granulosa cells and regulates mitosis by controlling both the rate at which cells enter the G₁ stage of the cell cycle and the successful completion of the metaphase. Furthermore, PGRMC2 plays a role in the P4 signal cascade that suppresses the rate of granulosa cell mitosis and apoptosis. Its precise role in this cascade is yet to be defined, but it is likely that PGRMC2 plays a role distal to P4 binding because depleting PGRMC2 does not alter ³H-P4 binding to SIGCs. Given that PGRMC2 is expressed in granulosa cells of developing ovarian follicles and influences the rate of both mitosis and apoptosis, PGRMC2 appears to be positioned to play an important role in regulating ovarian follicle development, justifying further studies on PGRMC2's mechanism of action.

ACKNOWLEDGMENT

The authors would like to acknowledge Dr. Martin Wehling of the University of Heidelberg-Mannheim for providing the GFP-PGRMC2 expression vector and Dr. Robert Burghardt of Texas A&M University for providing the spontaneously immortalized granulosa cells.

REFERENCES

1. Buffer G, Roser S. New data concerning the role played by progesterone in the control of follicular growth in the rat. *Acta Endocrinol (Copenh)* 1974; 75:569–578.
2. Chaffkin LM, Luciano AA, Peluso JJ. Progesterone as an autocrine/paracrine regulator of human granulosa cell proliferation. *J Clin Endocrinol Metab* 1992; 75:1404–1408.
3. Chaffkin LM, Luciano AA, Peluso JJ. The role of progesterone in regulating human granulosa cell proliferation and differentiation in vitro. *J Clin Endocrinol Metab* 1993; 76:696–700.
4. diZerega GS, Hodgen GD. The interovarian progesterone gradient: a spatial and temporal regulator of folliculogenesis in the primate ovarian cycle. *J Clin Endocrinol Metab* 1982; 54:495–499.
5. Kim I, Greenwald GS. Stimulatory and inhibitory effects of progesterone on follicular development in the hypophysectomized follicle-stimulating hormone/luteinizing hormone-treated hamster. *Biol Reprod* 1987; 36:270–276.
6. Lodde V, Peluso JJ. A novel role for progesterone and progesterone receptor membrane component 1 in regulating spindle microtubule stability during rat and human ovarian cell mitosis. *Biol Reprod* 2011; 84:715–722.
7. Moore PJ, Greenwald GS. Effect of hypophysectomy and gonadotropin treatment on follicular development and ovulation in the hamster. *Am J Anat* 1974; 139:37–48.
8. Peluso JJ, Leiper S, Steger RW. Effects of PGF₂ alpha-induced luteolysis and progesterone on follicular growth in pregnant mice. *Prostaglandins* 1980; 19:437–447.
9. Peluso JJ, Pappalardo A. Progesterone mediates its anti-mitogenic and anti-apoptotic actions in rat granulosa cells through a progesterone-binding protein with gamma aminobutyric acidA receptor-like features. *Biol Reprod* 1998; 58:1131–1137.
10. Park OK, Mayo KE. Transient expression of progesterone receptor messenger RNA in ovarian granulosa cells after the preovulatory luteinizing hormone surge. *Mol Endocrinol* 1991; 5:967–978.
11. Park-Sarge OK, Mayo KE. Regulation of the progesterone receptor gene by gonadotropins and cyclic adenosine 3',5'-monophosphate in rat granulosa cells. *Endocrinology* 1994; 134:709–718.
12. Park-Sarge OK, Parmer TG, Gu Y, Gibori G. Does the rat corpus luteum express the progesterone receptor gene? *Endocrinology* 1995; 136:1537–1543.
13. Peluso JJ, Fernandez G, Pappalardo A, White BA. Membrane-initiated events account for progesterone's ability to regulate intracellular free calcium levels and inhibit rat granulosa cell mitosis. *Biol Reprod* 2002; 67:379–385.
14. Peluso JJ, Pappalardo A, Losel R, Wehling M. Progesterone membrane receptor component 1 expression in the immature rat ovary and its role in mediating progesterone's antiapoptotic action. *Endocrinology* 2006; 147:3133–3140.
15. Peluso JJ, Romak J, Liu X. Progesterone receptor membrane component-1 (PGRMC1) is the mediator of progesterone's antiapoptotic action in spontaneously immortalized granulosa cells as revealed by PGRMC1 small interfering ribonucleic acid treatment and functional analysis of PGRMC1 mutations. *Endocrinology* 2008; 149:534–543.
16. Peluso JJ, Liu X, Gawkowska A, Johnston-MacAnanny E. Progesterone activates a progesterone receptor membrane component 1-dependent mechanism that promotes human granulosa/luteal cell survival but not progesterone secretion. *J Clin Endocrinol Metab* 2009; 94:2644–2649.
17. Peluso JJ, Liu X, Gawkowska A, Lodde V, Wu CA. Progesterone inhibits apoptosis in part by PGRMC1-regulated gene expression. *Mol Cell Endocrinol* 2010; 320:153–161.
18. Gerdes D, Wehling M, Leube B, Falkenstein E. Cloning and tissue expression of two putative steroid membrane receptors. *Biol Chem* 1998; 379:907–911.
19. Cahill MA. Progesterone receptor membrane component 1: an integrative review. *J Steroid Biochem Mol Biol* 2007; 105:16–36.
20. Nilsson EE, Stanfield J, Skinner MK. Interactions between progesterone and tumor necrosis factor-alpha in the regulation of primordial follicle assembly. *Reproduction* 2006; 132:877–886.
21. Skiadas CC, Duan S, Correll M, Rubio R, Karaca N, Ginsburg ES, Quackenbush J, Racowsky C. Ovarian reserve status in young women is associated with altered gene expression in membrana granulosa cells. *Mol Hum Reprod* 2012; 18:362–371.
22. Stein LS, Stoica G, Tilley R, Burghardt RC. Rat ovarian granulosa cell culture: a model system for the study of cell-cell communication during multistep transformation. *Cancer Res* 1991; 51:696–706.
23. Sakaue-Sawano A, Kurokawa H, Morimura T, Hanyu A, Hama H, Osawa H, Kashiwagi S, Fukami K, Miyata T, Miyoshi H, Imamura T, Ogawa M, et al. Visualizing spatiotemporal dynamics of multicellular cell-cycle progression. *Cell* 2008; 132:487–498.
24. Albrecht C, Huck V, Wehling M, Wendler A. In vitro inhibition of SKOV-3 cell migration as a distinctive feature of progesterone receptor membrane component type 2 versus type 1. *Steroids* 2012; 77:1543–1550.
25. Peluso JJ, DeCervo J, Lodde V. Evidence for a genomic mechanism of action for progesterone receptor membrane component-1. *Steroids* 2012; 77:1007–1012.
26. Peluso JJ, Yuan A, Liu X, Lodde V. Plasminogen activator inhibitor 1 RNA binding protein interacts with progesterone receptor membrane component 1 to regulate progesterone's ability to maintain the viability of spontaneously immortalized granulosa cells and rat granulosa cells. *Biol Reprod* 2013; 88:20.
27. Xiang J, Lahti JM, Grenet J, Easton J, Kidd VJ. Molecular cloning and expression of alternatively spliced PITSLRE protein kinase isoforms. *J Biol Chem* 1994; 269:15786–15794.
28. Zhang L, Kanda Y, Roberts DJ, Ecker JL, Losel R, Wehling M, Peluso JJ, Pru JK. Expression of progesterone receptor membrane component 1 and its partner serpine 1 mRNA binding protein in uterine and placental tissues of the mouse and human. *Mol Cell Endocrinol* 2008; 287:81–89.
29. Keator CS, Mah K, Slayden OD. Alterations in progesterone receptor membrane component 2 (PGRMC2) in the endometrium of macaques afflicted with advanced endometriosis. *Mol Hum Reprod* 2012; 18:308–319.
30. Kowalik MK, Slonina D, Rekawiecki R, Kotwica J. Expression of progesterone receptor membrane component (PGRMC) 1 and 2, serpine mRNA binding protein 1 (SERBP1) and nuclear progesterone receptor (PGR) in the bovine endometrium during the estrous cycle and the first trimester of pregnancy. *Reprod Biol* 2013; 13:15–23.
31. Saint-Dizier M, Sandra O, Ployart S, Chebrou M, Constant F. Expression of nuclear progesterone receptor and progesterone receptor membrane components 1 and 2 in the oviduct of cyclic and pregnant cows during the post-ovulation period. *Reprod Biol Endocrinol* 2012; 10:76.
32. Shankar R, Johnson MP, Williamson NA, Cullinane F, Purcell AW, Moses EK, Brennecke SP. Molecular markers of preterm labor in the choriodecidual. *Reproduct Sci* 2010; 17:297–310.
33. Maeda Y, Ohtsuka H, Tomioka M, Oikawa M. Effect of progesterone on Th1/Th2/Th17 and regulatory T cell-related genes in peripheral blood mononuclear cells during pregnancy in cows. *Vet Res Commun* 2013; 37:43–49.
34. Causey MW, Huston LJ, Harold DM, Charaba CJ, Ippolito DL, Hoffer ZS,

- Brown TA, Stallings JD. Transcriptional analysis of novel hormone receptors PGRMC1 and PGRMC2 as potential biomarkers of breast adenocarcinoma staging. *J Surg Res* 2011; 171:615–622.
35. Intlekofer KA, Petersen SL. 17beta-estradiol and progesterone regulate multiple progestin signaling molecules in the anteroventral periventricular nucleus, ventromedial nucleus and sexually dimorphic nucleus of the preoptic area in female rats. *Neuroscience* 2011; 176:86–92.
 36. Intlekofer KA, Petersen SL. Distribution of mRNAs encoding classical progestin receptor, progesterone membrane components 1 and 2, serpine mRNA binding protein 1, and progestin and ADIPOQ receptor family members 7 and 8 in rat forebrain. *Neuroscience* 2011; 172:55–65.
 37. Liu L, Wang J, Zhao L, Nilsen J, McClure K, Wong K, Brinton RD. Progesterone increases rat neural progenitor cell cycle gene expression and proliferation via extracellularly regulated kinase and progesterone receptor membrane components 1 and 2. *Endocrinology* 2009; 150:3186–3196.
 38. Bunnell BA, Heath LS, Adams DE, Lahti JM, Kidd VJ. Increased expression of a 58-kDa protein kinase leads to changes in the CHO cell cycle. *Proc Natl Acad Sci U S A* 1990; 87:7467–7471.
 39. Zong H, Chi Y, Wang Y, Yang Y, Zhang L, Chen H, Jiang J, Li Z, Hong Y, Wang H, Yun X, Gu J. Cyclin D3/CDK11p58 complex is involved in the repression of androgen receptor. *Mol Cell Biol* 2007; 27:7125–7142.
 40. Bartkova J, Lukas J, Strauss M, Bartek J. Cyclin D3: requirement for G1/S transition and high abundance in quiescent tissues suggest a dual role in proliferation and differentiation. *Oncogene* 1998; 17:1027–1037.
 41. Peluso JJ. Progesterone receptor membrane component 1 and its role in ovarian follicle growth. *Front Neurosci* 2013; 7:99.
 42. Thomas P, Pang Y, Dong J. Enhancement of cell surface expression and receptor functions of membrane progestin receptor alphas by progesterone receptor membrane component 1: evidence for a role of PGRMC1 as an adaptor protein for steroid receptors. *Endocrinology* 2014; 155: 1107–1119.